atoms

MDPI

Article

Data on Dissociative Electron Attachment Accommodated in the Structure of Belgrade Collisional Database ACol

Veljko Vujčić [1,*], Bratislav P. Marinković [2,*], Janina Kopyra [3], Jelena B. Maljković [2], Vladimir A. Srećković [2], Sanja Tošić [2], Nenad Aničić [4] and Nigel J. Mason [5]

1 Astronomical Observatory, Volgina 7, 11060 Belgrade, Serbia
2 Institute of Physics Belgrade, University of Belgrade, Pregrevica 118, 11080 Belgrade, Serbia; jelenam@ipb.ac.rs (J.B.M.); vlada@ipb.ac.rs (V.A.S.); seka@ipb.ac.rs (S.T.)
3 Faculty of Sciences, Siedlce University, 3 Maja 54, 08-110 Siedlce, Poland; janina.kopyra@uws.edu.pl
4 Faculty of Organizational Sciences, Jove Ilića 54, 11010 Belgrade, Serbia; anicic.nenad@fon.bg.ac.rs
5 School of Physics and Astronomy, University of Kent, Canterbury CT2 7NH, UK; n.j.mason@kent.ac.uk
* Correspondence: veljko@aob.rs (V.V.); bratislav.marinkovic@ipb.ac.rs (B.P.M.)

Abstract

This work presents an extension of the Belgrade ACol collisional database within the Virtual Atomic and Molecular Data Centre (VAMDC) framework to include dissociative electron attachment (DEA) processes. DEA, a low-energy electron-driven resonant mechanism leading to molecular fragmentation, is relevant in fields such as plasma science, radiation damage, nanofabrication, and EUV lithography. The ACol data model was redesigned to improve semantic clarity and flexibility by separating physical collision data from bibliographic and serialization structures. A new DataSource entity and a redefined TabulatedData–Collision relationship enable a more normalized database while preserving compatibility with the XSAMS schema through dynamic, query-time construction of hierarchical structures. The implementation is demonstrated using DEA to isoflurane, incorporating experimental data from independent studies and cataloging resulting fragment anions and energy-dependent yields. Elastic cross sections of isoflurane are included as they are immanently connected to DEA, providing an essential tool for understanding the complex DEA process. The novelty of the present implementation lies not in the first representation of DEA within VAMDC, but in its integration into a multi-process collision database based on a compact, normalized data model that separates scientific data and bibliographic provenance from the XSAMS serialization structure. The updated architecture enhances interoperability, reduces redundancy, and improves data management while maintaining compliance with VAMDC standards.

Keywords: collisional database; dissociative electron attachment; isoflurane; VAMDC; XSAMS; electron–molecule collisions; data model

Check for updates

Academic Editor: Nidhi Sinha

Received: 2 May 2026
Revised: 2 July 2026
Accepted: 7 July 2026
Published: 9 July 2026

Copyright: © 2026 by the authors. Licensee MDPI, Basel, Switzerland. This article is an open access article distributed under the terms and conditions of the Creative Commons Attribution (CC BY) license.

1. Introduction

In this paper, we discuss improvements made to the collisional database ACol, which is one of the Belgrade nodes within the Virtual Atomic and Molecular Data Centre (VAMDC). The VAMDC Consortium [1,2] is an association of 39 independently maintained and curated databases in the field of atomic, molecular, and optical physics whose member databases contain data on elementary collisional and radiative processes, including their cross sections, rates, and energy dependencies, as well as elementary data such as wavelengths, optical strengths, transition probabilities, etc. The existence of such databases is essential for

both data providers and data users, since as they provide a reliable, centralized source of scientific data that would otherwise be dispersed across myriad scientific publications. Such databases facilitate research in many disparate areas, for example, in models and observations of the interstellar medium and planetary atmospheres [3] or in the analysis of experiments using swarm techniques [4].

The purpose of this work is to extend the coverage of collisional processes currently represented in ACol [5]. Beyond the five processes, namely, excitation, associative ionization, dissociative recombination, electron–ion–atom recombination, and Penning ionization, we now include the process called Dissociative Electron Attachment (DEA). The DEA process is relevant at low electron impact energies, where an electron interacting with a molecule forms a temporary negative ion (TNI). This is a resonant process, highly dependent on the electron impact energy, such that the TNI is also known as a resonance. Such a resonance is a short-lived species that dissociates into an anion and neutral fragment(s). Alternatively, the TNI can re-emit the electron and thus return to elastic scattering. The competing process is spontaneous electron detachment (autodetachment) [6,7]. That is why it is always important to study the elastic scattering process in addition to DEA. Elastic electron scattering experiments are used to detect the resonances that are required in DEA so that electrons may be captured at specific energy levels. Theoretical descriptions of DEA rely extensively on elastic electron–molecule scattering data. The cross section of a molecule undergoing DEA is deeply tied to the temporary trapping and scattering potentials of the target molecule.

Beyond its resonant nature, DEA is characterized by pronounced bond and site selectivity. For isolated molecules, electron attachment is strongly influenced by both the symmetry properties of the chemical bonds and the spatial arrangement of the constituent atoms. Dissociation can occur via either a direct pathway, arising from the population of repulsive σ^* states, or an indirect predissociation mechanism involving transient occupation of π^* orbitals. Depending on the initial electron energy and electron affinity of the molecule, TNIs may be classified as single-particle shape resonances, core-excited shape resonances, or core-excited Feshbach resonances. A comprehensive review of the various types of DEA processes, their underlying molecular mechanisms, and representative examples illustrating their selectivity is provided in [7].

Given the importance of the DEA process, dedicated DEA Club meetings are held biennially or triennially. An overview of contemporary research activities within the DEA community is provided in the report of the fourth DEA Club meeting [8]. The inclusion of DEA processes in the ACol database was motivated by discussions at the fifth DEA Club Meeting, held in 2026 in Sopot, Poland, which highlighted the need for their systematic development and integration [9].

Current studies of the DEA process include many important fields, including technological plasmas, radiation damage (RADAM), microhydrated radiosensitizers, focused electron beam-induced processing (FEBIP), and EUV lithography. A schematic illustration of different aspects of the DEA process is presented in Figure 1. The role of DEA in RADAM has been well established since 2000, when the group of Leon Sanche [10] showed that low-energy electrons may cause single- and double-strand breaks in the DNA helix via the DEA process. Recently, the complexity of DNA radiation damage has been investigated using DNA nanotechnology, illuminating the role of DEA in DNA fragmentation [11]. Radiosensitizers are molecules that increase DNA susceptibility to radiation-induced damage, which is extremely important under hypoxic conditions. The recent perspective article [12] reviews both established candidate radiosensitizers and promising future directions in radiosensitizer development. Radiosensitizing nucleosides include uracil-based derivatives or novel purine-based derivatives [13] that undergo DEA, yielding DNA strand breaks.

Recent advances have highlighted the broader role of DEA processes in the design and optimization of radiosensitizers for biomedical applications. A comprehensive review by Sedmidubská and Kočišek [12] summarizes current experimental and theoretical studies of low-energy electron interactions with radiosensitizing molecules and discusses their implications for enhancing radiation-induced DNA damage. Extensive experimental and theoretical studies are also being performed on electron attachment to different molecules and clusters, both in the gas and hydrated phases [14,15]. In FEBIP, low-energy electrons play a pivotal role, with DEA inducing the dissociation of precursor molecules and forming nanostructures [6,16]. Acid generator resists for EUV lithography, operating at 13.5 nm wavelength, have been recently proposed that exploit DEA and its ability to selectively fragment molecules [17].

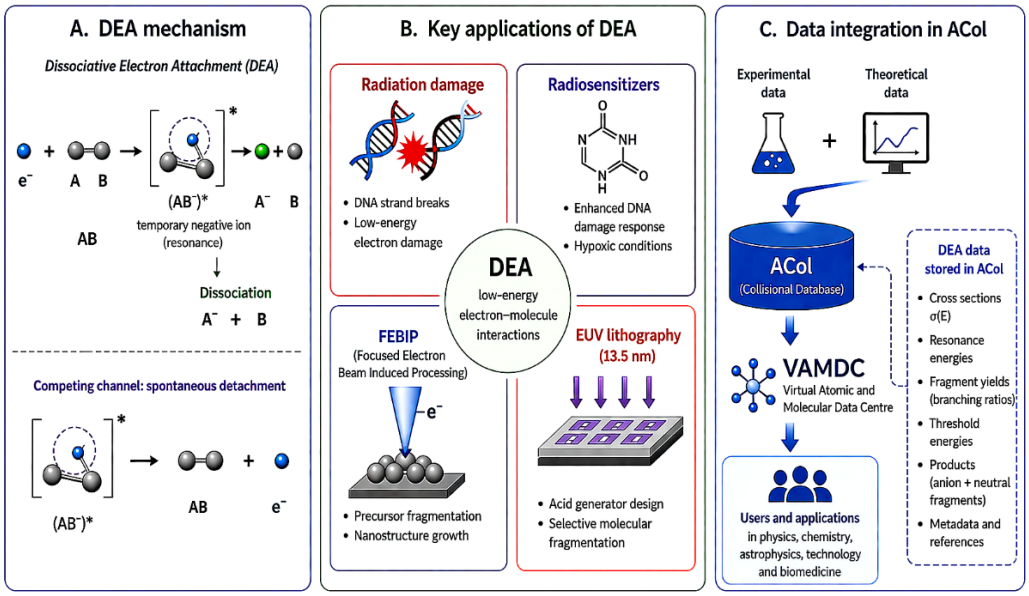


Figure 1. Schematic illustration of the dissociative electron attachment (DEA) mechanism where * indicates a resonance state (**A**), its major scientific and technological applications (**B**), and the integration of experimental and theoretical DEA data into the ACol database within the VAMDC infrastructure (**C**).

Although it has been known since 2021 that the VAMDC infrastructure can accommodate DEA data, when the Innsbruck Dissociative Electron Attachment Database (IDEADB) was established [18], it has remained an open question whether the Belgrade VAMDC nodes could also support this type of data. From the perspective of reaction databases, in addition to VAMDC, the LXCat project provides a repository of cross-section data for reactions needed to model electron and ion swarm parameters in non-equilibrium low-temperature plasmas [19]. The main processes covered are elastic electron scattering, electron impact excitation, and ionization. However, a complete database representation of electron and ion kinetics would require the inclusion of additional reaction types and processes, including DEA [20]. Such an extension requires the definition of a new data format, the selection of an appropriate database type, and the design of the software stack [21]. These findings underscore the importance of incorporating DEA processes into reaction databases to enable more comprehensive kinetic modeling.

DEA may produce several chemically distinct anion fragment channels from the same parent molecule, each associated with a separate energy-dependent yield and ion mass [22]. Database representation therefore requires explicit identification of individual ionic products and a serialization mechanism capable of returning multiple ion species within the appropriate XSAMS atomic structure. It appears natural that the Belgrade electron/atom

(molecule) database (BEAM) [5] should accommodate the DEA process since one of the reactants is always an electron. However, another Belgrade node, ACol, Collisional Atomic Processes (Excitation–Ionization), was selected to host the DEA data because its reactant product structure is better suited to representing multiple fragmentation channels. In this paper, we present how the ACol database has incorporated DEA data. Isoflurane was selected as an initial case study due to the availability of recent measurements in which DEA data were independently obtained by two separate research groups [23,24].

2. Methods Used to Describe DEA Process in ACol Database

2.1. DEA to the Volatile Halogenated Anesthetics

Studies of volatile halogenated anesthetics are important because of their prevalence in clinical practice [25]. There is also concern about their contribution to global warming since they have a long lifetime in the atmosphere and a relatively high global warming potential (GWP) [26]. Experimental studies on the DEA process were carried out using monochromatic electron beams in a crossed-beam arrangement with mass spectrometers, either two-sector field mass spectrometers [23] or conventional quadrupole mass analyzers [24], to detect the anion fragments.

Isoflurane (CF_3–CHCl–O–CHF_2) is designated as 2-chloro-2-(difluoromethoxy)-1,1,1-trifluoroethane according to IUPAC nomenclature, but it can also be regarded as 1-chloro-2,2,2-trifluoroethyl difluoromethyl ether. All hydrofluoroethers strongly absorb in the VUV region. Absorption cross sections have been measured for isoflurane in the range from 5.0 eV to 10.8 eV (115–248 nm) [27], while infrared spectra have recently been measured in the range from 1650 to 650 cm^{-1} [26]. Reactions with hydroxyl (OH·) radicals are generally used to elucidate the GWP of hydrofluoroethers as long-lived species [28].

2.2. Modifications of ACol Data Model and Schema Generation

The ACol [5] database and service, hosted by the Serbian Virtual Observatory[1] is a VAMDC [1] node that operates within the broader ecosystem of heterogeneous, interoperable data nodes with a unified web service and centralized portal access. The implementation of a VAMDC node is typically derived from the upstream version of the NodeSoftware[2], which provides a common framework for data access and XSAMS [29,30] XML serialization. Individual nodes incorporate specific data models and a range of customizations to accommodate the structure and semantics of their underlying datasets, while conforming to the serialization standard.

We revised the ACol data model and retrieval workflow to support DEA data within the existing multiprocess structure of the database while preserving compatibility with the VAMDC XSAMS standard. The updated organization separates the physical description of collision processes, numerical datasets, and bibliographic provenance more clearly, allowing multiple reaction channels and independent measurements to be represented consistently without unnecessary duplication. Figure 2 provides an overview of the principal database entities and their relationships. A detailed description of the database refactoring, relationships between individual entities, and the extended XSAMS serialization procedure is provided in Appendix A. This revision of the software exhibits a cleaner separation between domain semantics and serialization concerns, reduces redundancy, and leverages dynamic composition to bridge the gap between an optimized relational model and a rigid external XML schema.

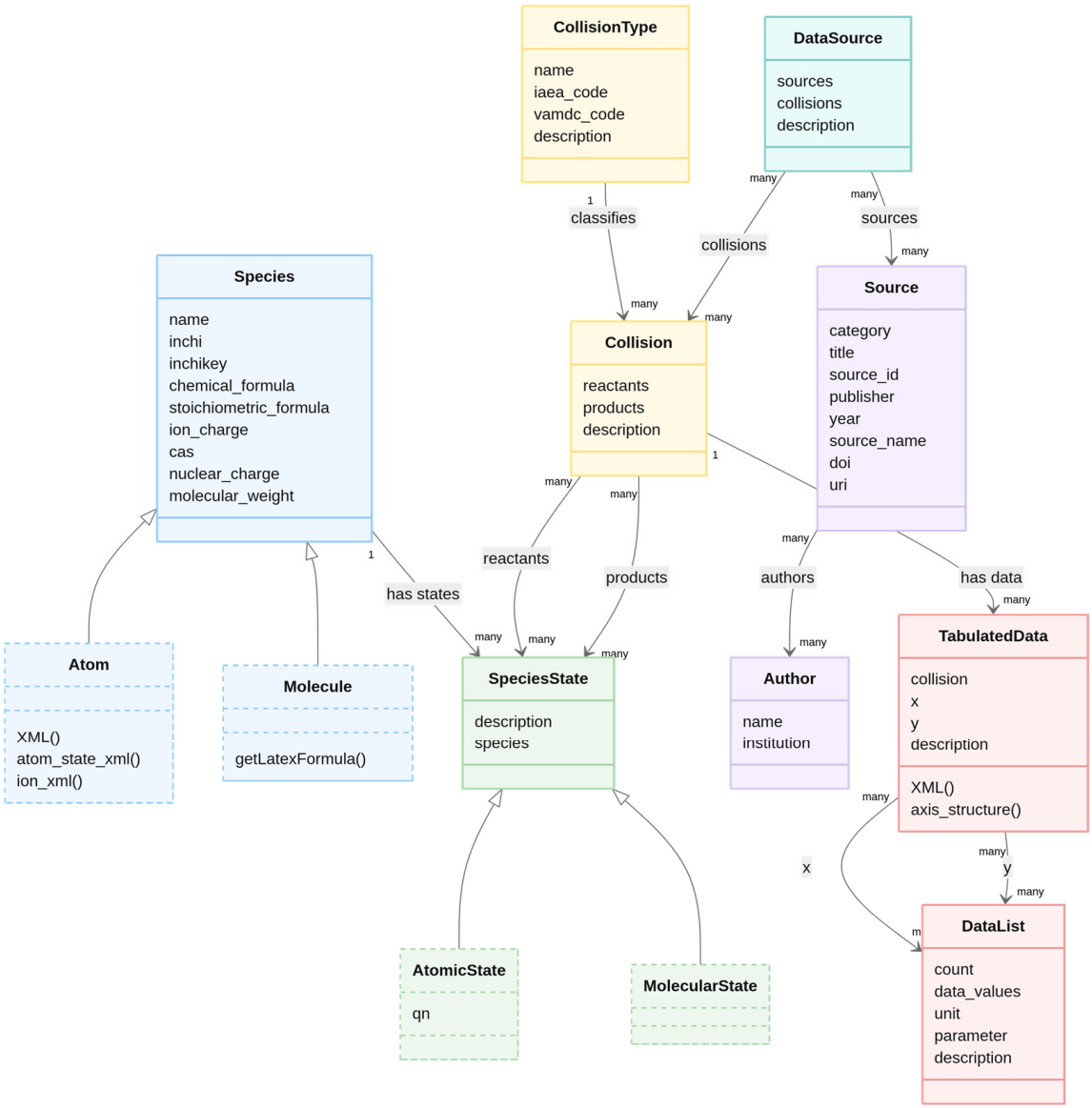


Figure 2. Class diagram of the ACol data model.

The overall ACol workflow is summarized in Figure 3. The web interface and external VAMDC clients provide two distinct access paths to the same underlying relational database. Browser-based functions, including the newly introduced Overview dashboard and Explore Data tools, as well as the qn plots, are handled through dedicated Django views that return statistics, filtered dataset descriptions, source metadata, raw numerical values, and plot output. Standardized data retrieval is performed through the VAMDC-TAP endpoint, where VSS2 queries are translated through the node dictionaries and query functions into database operations before the results are serialized as XSAMS XML. Both paths rely on the same normalized persistence layer, while the XSAMS-specific hierarchical structures are constructed dynamically during query processing rather than stored directly in the database.

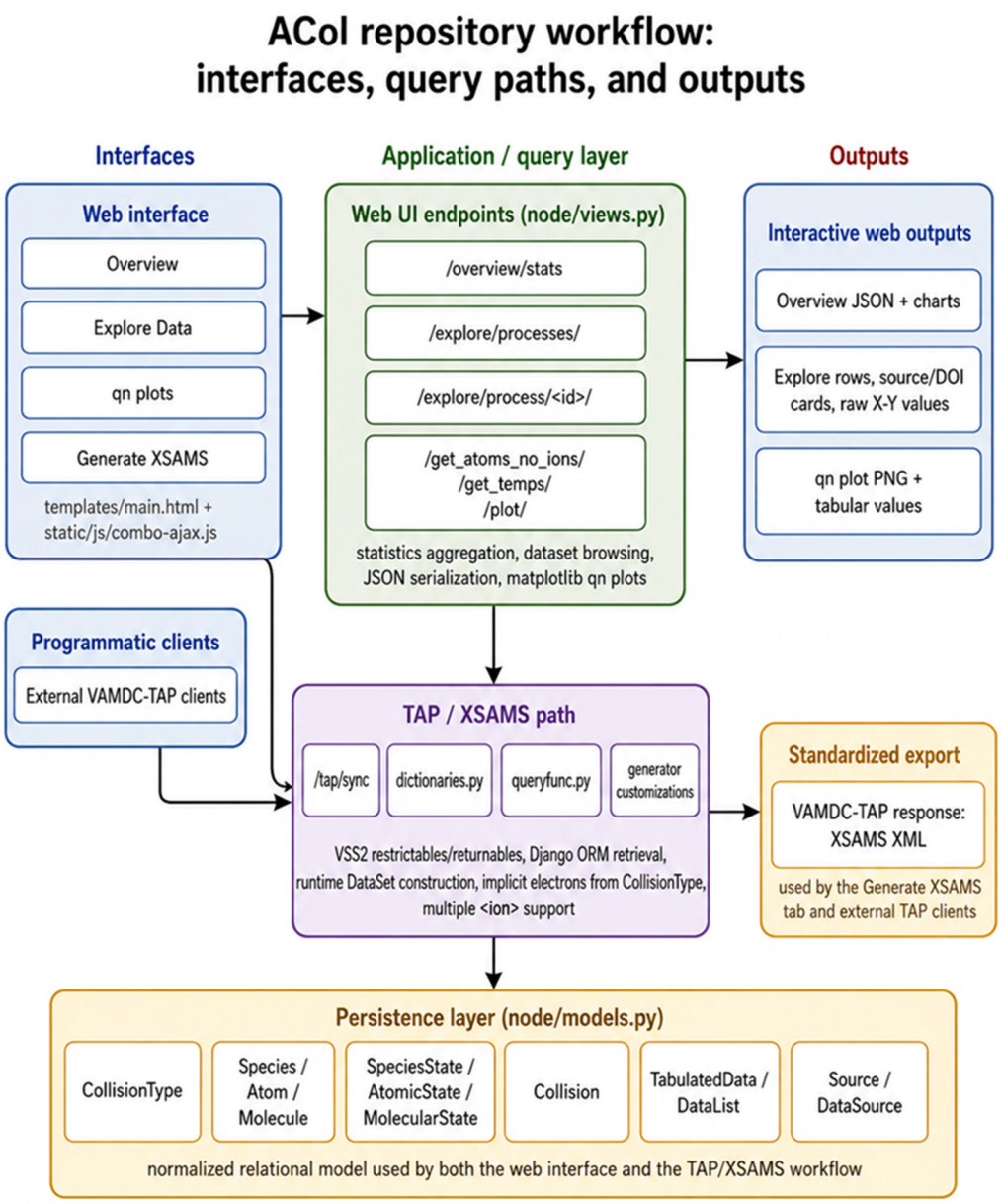


Figure 3. Repository-based workflow showing how ACol serves browser users through JSON and plotting endpoints, and VAMDC clients through/`tap/sync`, while both paths rely on the same normalized collision database.

2.3. Database Access, Curation, and Data Quality

ACol is a curator-managed database rather than an open repository in which users directly upload records. New datasets are selected and entered by the ACol team, generally from peer-reviewed publications or through direct collaboration with data producers. Scientists may propose additional datasets or provide numerical data and metadata to the authors, but the final mapping of species, states, reaction channels, units, sources, and tabulated values is performed by the database curators.

Validation is carried out at two levels. First, the database representation is checked for technical consistency, including species identity, charge and mass information, reactant product assignments, units, the declared number of numerical values, relations between database objects, and successful XSAMS serialization. Second, the entered numerical arrays and bibliographic metadata are compared with the original publication, and graphical inspection is used to identify transcription errors, discontinuities, or incorrect unit assign-

ments. This procedure verifies the faithful representation of the published data but does not constitute an independent experimental or theoretical reassessment of the source results.

Uncertainties are not generated or estimated by ACol; they must originate from the source publication. The present data model stores the reported independent and dependent numerical values, their units, descriptions, and bibliographic provenance, but does not yet provide a dedicated machine-readable array for point-wise uncertainties. Where uncertainty information is available, users should consult the linked original publication. The structured representation of uncertainties and additional experimental metadata is a possible extension of the data model.

3. Results

3.1. Data on DEA to Isoflurane Molecule

We have used the results of DEA for the isoflurane molecule obtained by two independent groups of researchers [23,24] as a case study. Within the entity *Sources,* all relevant data from the publication are listed: title, type of publication, all authors, year of publication, volume, page range, unique identifier, and digital object identifier. Within a class *Species,* both reactants and products are specified. One of the reactants is always a particle, in this case an electron, while the other is a molecule defined with its ordinary structural formula, stoichiometric formula, ion charge, chemical name, InChI, and InChIKey. Additionally, a description of the molecular state is provided; however, in the present work, only the ground state is considered. Within the *Processes* entity, there are two distinct paths, radiative and collisional. Collisional transitions are distinguished by a unique ID. The process itself is a class with its name, VAMDC code, and IAEA code. Data sets for DEA comprise two axes, X as electron energy and Y as anion yield. Selected fragment anions from DEA to isoflurane are listed in Table 1 together with the values of *m/z* and peak maxima as identified in the literature. Here, we compare results reported in two independent studies: one conducted through a collaboration between the Innsbruck, Lisbon, and Birmingham research groups [23], and the other by the Siedlce and Belgrade research groups [24]. Datasets are imported into ACol in the form in which they are originally presented in the corresponding references. Consequently, no normalization is performed across datasets from different sources; any normalization is limited to that applied within individual references. The appearance of peak positions within ion yields is shown in the first two columns. Although the two datasets differ in the positions of certain peaks, they also share several common features. The uncertainty associated with the peak energy is estimated to be ± 0.2 eV, based on variations in the positions of the calibration peaks observed throughout the experiment. A comprehensive discussion of the comparison is provided in [24].

Table 1. Selected fragment anions from DEA to isoflurane presented in the ACol database. Positions of peak maxima in ion yields, the ion species and values of *m/z* are presented.

Kopyra et al. [24] (eV)	**Matias et al. [23] (eV)**	**Anion**	***m/z***
6.2 & >9	3.3 & 7.1 & 9.3	F^-	19
0.1	0.6 & 3.3 & 9.2 & 12.6	Cl^-	35
0.7 & 2.7	3.0 & 6.9 & 9.5	HF_2^-	39
0.7 & 2.6	3.0 & 9.3 & 13.1	CFO^-	47
1.9	2.9 & 9.2	CHF_2O^-	67
0.6 & 2.6	3.1	$C_2F_3Cl^-$	116

3.2. Data on Elastic Scattering by Isoflurane Molecule

Due to the role of isoflurane in clinical practice and its high global warming potential, extensive elastic electron scattering experiments and calculations have been performed [31]. Absolute differential cross sections (DCS) have been measured in a crossed-beam experiment for scattering angles from 25° to 125° and at electron impact energies from 50 eV to 300 eV. These data are deposited in the BEAM database. Calculations were performed using the Independent Atom Model and the Screening Corrected Additivity Rule with incorporated interference effects (IAM-SCAR + I). The theoretical DCS span more than five orders of magnitude, whereas the experimental data values span approximately three orders of magnitude, reflecting the fact that the data were acquired over a limited angular range. Experimental data are shown in Figure 4.

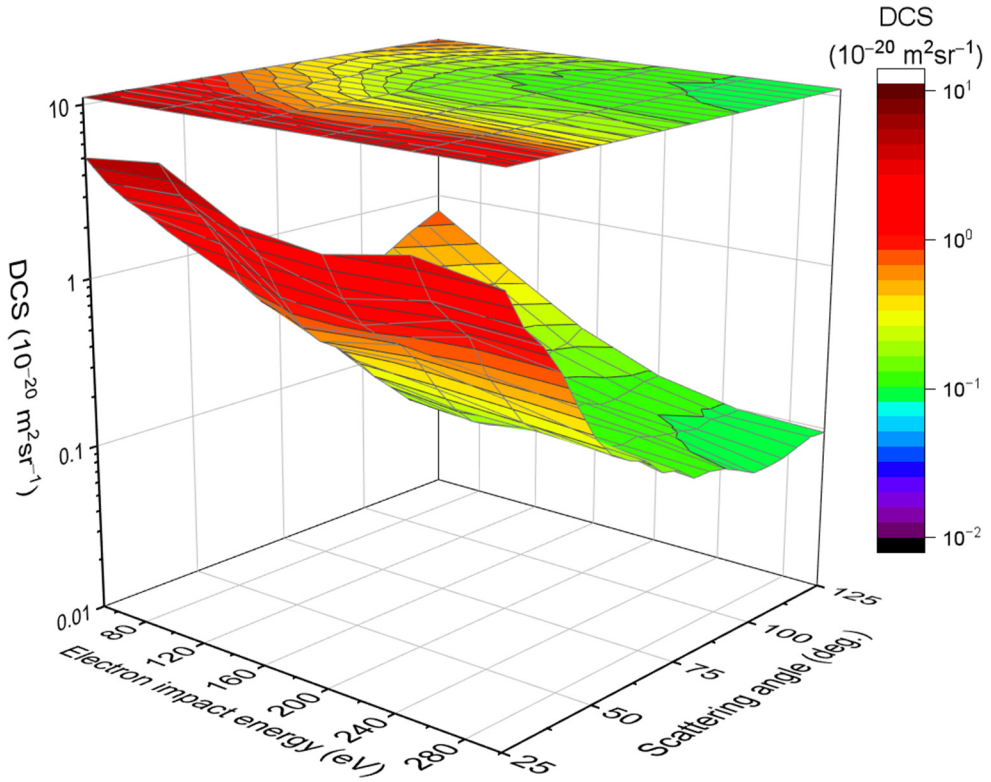


Figure 4. Differential cross sections for elastic electron scattering by isoflurane molecule (CF_3-CHCl–O–CHF_2) as a function of electron impact energy and scattering angle. Data captured from the BEAM database [31].

3.3. Representation in ACol Database

The revised ACol implementation improves both semantic consistency and operational flexibility. The numerical data are linked directly to the collision processes they describe, while bibliographic provenance is represented independently. The hierarchical objects required by XSAMS are not stored in the database; instead, they are created temporarily during query processing and serialization. This keeps the relational model compact while preserving full compatibility with the XSAMS output format.

Figure 5 presents the newly introduced ACol web interface used for browsing, inspecting, and retrieving atomic and molecular collision data. Whereas the previous interface was primarily oriented toward constructing queries and returning XSAMS output, the redesigned interface now supports direct, interactive exploration of the database before export. It includes an Overview dashboard with database statistics, an Explore Data section for live filtering by collision type, species, and bibliographic source, interactive

inspection of individual plots and tabulated datasets, and dedicated 'qn plots' for selected state-resolved processes.

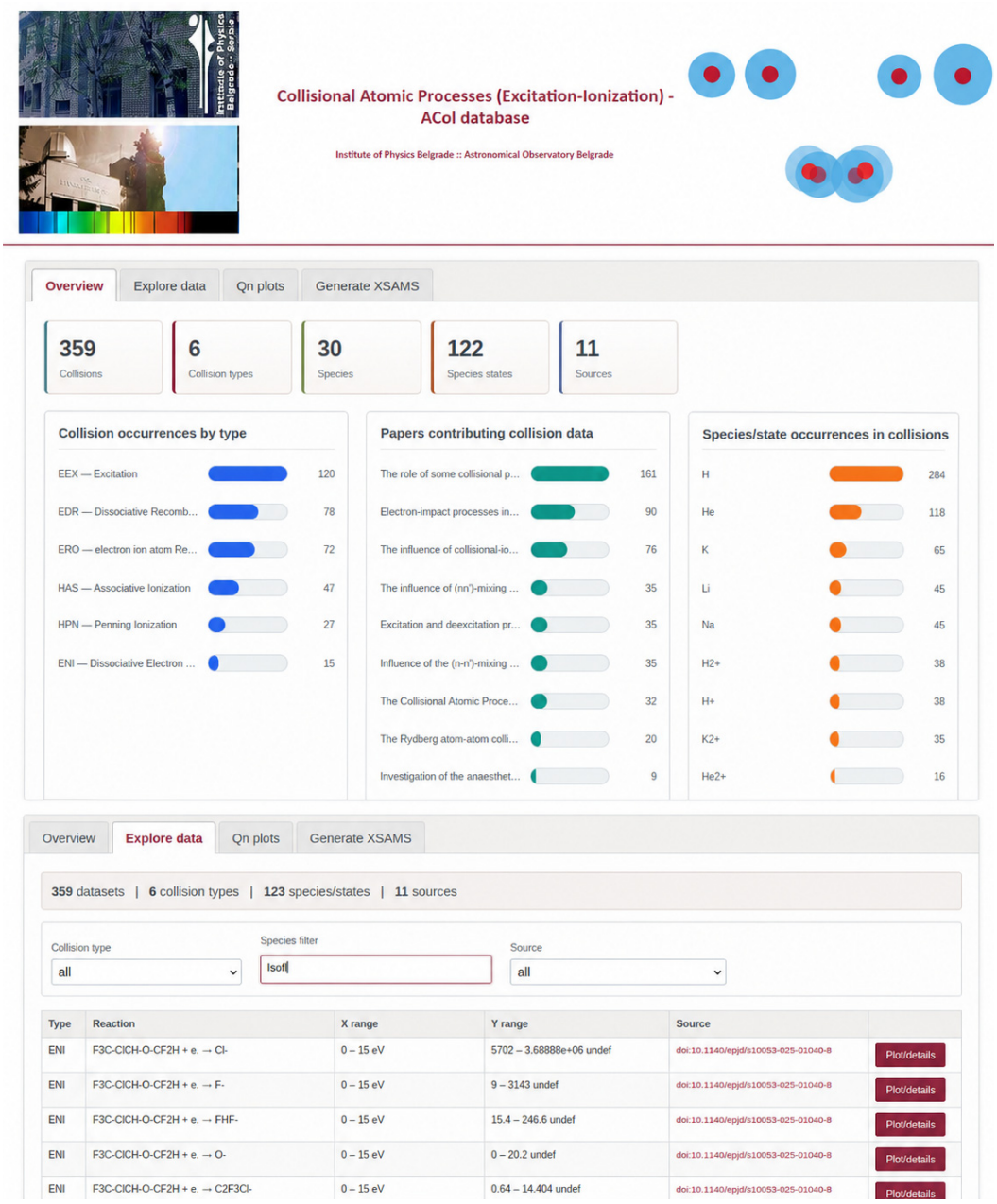


Figure 5. ACol web interface providing a search functionality for collisional data retrieval. Overview page showing database statistics and distributions of collision data by process type, source, and species/state occurrence. Explore data page providing access to collision datasets through filtering and search options, with links to detailed dataset information and graphical representations.

The Overview section provides a continuously updated summary of the scientific content currently available in ACol. It reports the total number of collisions, collision types, species, species states, and bibliographic sources, together with distributions of collision records by process type, contributing publication, and species/state occurrence. At the time of revision, ACol contained 359 collision records covering 6 collision types, 30 species, 122 species states, originating from 11 bibliographic sources.

This live overview complements the more detailed Explore Data interface and allows users to assess the scope and composition of the database before searching for individual

datasets. Users can examine reaction channels, numerical ranges, source titles, and DOI links, display plots together with tabulated raw X-Y values, and then generate XSAMS output for selected processes. The interface therefore extends ACol from a standards-compliant data endpoint into a practical scientific exploration environment.

The ACol database implementation, including its database schema, software architecture, configuration files, data models, interface components, and documentation, is publicly available through the GitHub (version 2.0.0) repository. A versioned release corresponding to the present work has also been archived on Zenodo to support reproducibility and long-term accessibility [32].

4. Conclusions and Future Directions

The integration of Dissociative Electron Attachment processes into the ACol database represents a significant extension of its scientific scope within the VAMDC infrastructure. By introducing a refined data model that separates physical collision data from bibliographic and structural elements, the database achieves improved semantic clarity, reduced redundancy, and greater flexibility in data management. The adoption of a runtime construction approach for XSAMS-compliant structures preserves interoperability while allowing a more normalized and efficient internal representation. The successful implementation using isoflurane as a case study demonstrates the practical applicability of the updated framework and confirms its ability to accommodate complex, energy-dependent electron-driven processes. Overall, these developments strengthen ACol's role as a robust and adaptable resource for collisional atomic and molecular data.

Future work on the database may focus, from a domain perspective, on further refinements of the data model to enable a more detailed treatment of molecular states, isotopologues, and excited-state dynamics. In addition, the range of supported collisional processes could be easily further extended beyond the currently implemented set.

From a technical perspective, the platform could be further enhanced as a data-intensive system through improvements in both data access and user interaction layers. This includes query-driven, interactive visualization components for efficient exploration of large collision datasets, as well as backend optimization of data retrieval and aggregation workflows. In addition, the data quality pipeline could be strengthened by combining rule-based validation at ingestion and API level with statistical and machine learning-based anomaly detection over stored data, improving consistency, reliability, and maintainability of the database at scale. Beyond quality assurance, the increasing availability of standardized DEA datasets may enable the development of predictive machine learning approaches for electron-driven molecular processes. Recent work has demonstrated the potential of machine learning methods for predicting and refining DEA properties and electron collision cross sections, including the prediction of DEA properties for halogenated molecules, highlighting the importance of interoperable, high-quality databases for supporting data-driven research in this field [33,34].

Author Contributions: All authors contributed equally to the writing and preparation of the manuscript. All authors have read and agreed to the published version of the manuscript.

Funding: This research was partially funded by the Science Fund of Serbia, grant number 6821. The Institute of Physics Belgrade, University of Belgrade, and Astronomical Observatory supported this work with grants from the Republic of Serbia's Ministry of Science, Technological Development, and Innovations.

Data Availability Statement: Data presented in this work are reposited in ACol and BEAM databases, available at http://servo.aob.rs/acol/ (accessed on 12 May 2026) and http://servo.aob.rs/emol/ (accessed on 12 May 2026). The corresponding software release is archived on Zenodo [32].

Acknowledgments: B.P.M., J.B.M., V.A.S. and S.T. acknowledge the support by Science Fund of Serbia, ATMOLCOL project #6821 "Atoms and (bio)molecules-dynamics and collisional processes on short time scale". J.K. acknowledges support by a statutory activity subsidy (No 201/26/B) from the Polish Ministry of Science and Higher Education. This contribution is also based on research from COST Action CA21101—Confined molecular systems: from a new generation of materials to the stars (COSY), supported by COST (European Cooperation in Science and Technology).

Conflicts of Interest: The authors declare no conflicts of interest.

Abbreviations

The following abbreviations are used in this manuscript:

ACol	Belgrade Collisional database
DEA	Dissociative Electron Attachment
XSAMS	XML Schema for Atoms, Molecules, and Solids
VAMDC	Virtual Atomic and Molecular Data Centre
TNI	Temporary Negative Ion
RADAM	Radiation Damage
FEBIP	Focused Electron Beam Induced Processing
IDEADB	Innsbruck Dissociative Electron Attachment Database
GWP	Global Warming Potential
InChI	The IUPAC International Chemical Identifier
InChIKey	A hashed version of the full InChI
IAEA	International Atomic Energy Agency
DCS	Differential Cross-Section
IAM-SCAR + I	Independent Atom Model and the Screening Corrected Additivity Rule with incorporated Interference effects
LXCat	ELECtron (and ion) SCATtering

Appendix A

The original ACol data model closely followed the legacy of the VAMDC XSAMS-oriented structure, in which the *DataSet* entity served as a central aggregation point linking collisions, sources, and tabulated data. In practice, this led to a semantic overload: each collisional transition required its own *DataSet* instance even when multiple transitions originated from the same bibliographic source. This resulted in unnecessary duplication and a loss of conceptual clarity, as the *DataSet* class simultaneously represented both a physical dataset (e.g., from a paper) and an XML structural container nested within an individual collisional process.

Refactoring introduced a clear separation of concerns within the data layer. As shown in the class diagram, *TabulatedData* now maps many-to-one to the entity *Collision*, establishing an explicit and physically meaningful mapping between numerical values and the process they describe. In parallel, a new *DataSource* entity was introduced to model the many-to-many relationship between *Source* and *Collision*, effectively capturing the notion of a bibliographic or experimental grouping of data independent of XSAMS serialization requirements. This restructuring normalizes the database structure and aligns the schema more closely with the underlying scientific semantics; moreover it reduces steps in the administrative workflow and the input of new datasets (see Figure 2).

At the same time, the XSAMS generation requirements still expect a hierarchical *DataSet*→*TabulatedData* structure which was satisfied without reintroducing persistence-level complexity. Instead, the *DataSet* concept was demoted to a runtime construct assembled within the query layer. As indicated in the diagram, TabulatedData objects are grouped per collision and injected into *coll.DataSets* during query processing, effectively

emulating the expected XSAMS hierarchy. This approach allows the persistence model to remain normalized while maintaining compatibility with the external schema.

The many-to-many relationships, in which each record on either side may be linked to multiple records on the other, are particularly useful for DEA data because the same molecular state may participate in several fragmentation channels, while a single publication may report measurements for several distinct fragment anions. In the revised model, reactants and products are linked to *Collision* through many-to-many relations with *SpeciesState*, so that species definitions are reused rather than duplicated for each process. Bibliographic provenance is handled independently through *DataSource*, which may associate several Source records with several *Collision* records. At the same time, each *TabulatedData* object is linked directly to the physical collision that it describes. This arrangement allows multiple energy-dependent yield curves and independent measurements to be stored without conflating the reaction channel, the numerical data, and the publication from which the data originate.

In the Atom class, we made an override of the default XML generation to construct an atomic structure explicitly, including not only ion grouping but also the iterative generation of multiple <Ion> elements within a single <Atom>. A simplified example is shown below within Listing A1:

Listing A1. Simplified XSAMS representation of multiple ionic stages within a single atomic structure.

```
<Atom>
  <ChemicalElement>
    <ElementSymbol>He</ElementSymbol>
  </ChemicalElement>
  <Isotope>
    <Ion speciesID="...">
      <IonCharge>0</IonCharge>
    </Ion>
    <Ion speciesID="...">
      <IonCharge>1</IonCharge>
    </Ion>
  </Isotope>
</Atom>
```

This represents an extension over the upstream NodeSoftware version, where support for multiple ions per element, while supported in the formal XSAMS definition, was effectively absent in implementation. The customized logic introduces a loop over dynamically attached ion instances, enabling the presentation of a complete ionic structure for a given species. While the XSAMS schema also allows a further level of hierarchy through isotopes, this was deliberately not introduced at this stage in order to avoid unnecessary complexity in both the data model and query layer.

Notes

[1] http://servo.aob.rs/acol, accessed on 12 May 2026.
[2] https://github.com/VAMDC/NodeSoftware, the release 12.07, accessed on 12 May 2026.

References

1. Dubernet, M.L.; Antony, B.K.; Ba, Y.A.; Babikov, Y.L.; Bartschat, K.; Boudon, V.; Braams, B.J.; Chung, H.-K.; Daniel, F.; Delahaye, F.; et al. The virtual atomic and molecular data centre (VAMDC) consortium. *J. Phys. B* **2016**, *49*, 074003. [CrossRef]
2. Albert, D.; Antony, B.K.; Ba, Y.A.; Babikov, Y.L.; Bollard, P.; Boudon, V.; Delahaye, F.; Del Zanna, G.; Dimitrijević, M.S.; Drouin, B.J.; et al. A Decade with VAMDC: Results and Ambitions. *Atoms* **2020**, *8*, 76. [CrossRef]
3. Marinković, B.P.; Srećković, V.A.; Dujko, S.; Tošić, S.; Maljković, J.B.; Vujčić, V.; Mason, N.J. Collisional ionization data for research of interstellar medium and planetary atmospheres. *Phys. Scr.* **2025**, *100*, 072002. [CrossRef]
4. Casey, M.J.E.; Stokes, P.W.; Cocks, D.G.; Bošnjaković, D.; Simonović, I.; Brunger, M.J.; Dujko, S.; Petrović, Z.L.; Robson, R.E.; White, R.D. Foundations and interpretations of the pulsed-Townsend experiment. *Plasma Sources Sci. Technol.* **2021**, *30*, 035017. [CrossRef]
5. Srećković, V.A.; Marinković, B.P.; Ignjatović, L.M.; Vujčić, V. MolD, EMol and Acol atomic and molecular databases for astrophysics: Current stage and new directions of development. *Contrib. Astron. Obs. Skaln. Pleso* **2025**, *55*, 81–87. [CrossRef]
6. May, O.; Kubala, D.; Allan, M. Dissociative electron attachment to $Pt(PF_3)_4$—A precursor for Focused Electron Beam Induced Processing (FEBIP). *Phys. Chem. Chem. Phys.* **2012**, *14*, 2979–2982. [CrossRef] [PubMed]
7. Bald, I.; Langer, J.; Tegeder, P.; Ingólfsson, O. From isolated molecules through clusters and condensates to the building blocks of life. *Int. J. Mass Spectrom.* **2008**, *277*, 4–25. [CrossRef]
8. Ameixa, J.; Fedor, J.; Bald, I.; Mason, N.; Ptasinska, S. Exploring dissociative electron attachment: Insights from the 4th DEA Club Meeting. *Eur. Phys. J. D* **2026**, *80*, 37. [CrossRef]
9. Janina Kopyra, J.; Śmiałek-Telega, M. (Eds.) *5th DEA Club Meeting 2026, 13–15 April 2026, Sopot, Poland: Book of Abstracts*; Gdansk Tech: Gdansk, Poland, 2026. Available online: https://cdn.files.pg.edu.pl/wimio/DEA%20CLUB%202026/DEA%202026%20BOOK%20OF%20ABSTRACTS.pdf (accessed on 12 May 2026).
10. Boudaiffa, B.; Cloutier, P.; Hunting, D.; Huels, M.A.; Sanche, L. Resonant formation of DNA strand breaks by extremely low energy (3–20 eV) electrons. *Science* **2000**, *287*, 1658–1660. [CrossRef] [PubMed]
11. Ameixa, J.; Bald, I. Unraveling the Complexity of DNA Radiation Damage Using DNA Nanotechnology. *Acc. Chem. Res.* **2024**, *57*, 1608–1619. [CrossRef] [PubMed]
12. Sedmidubská, B.; Kočišek, J. Interaction of low-energy electrons with radiosensitizers. *Phys. Chem. Chem. Phys.* **2024**, *26*, 9112–9136. [CrossRef] [PubMed]
13. Datta, M.; Szczyrba, A.; Zdrowowicz, M.; Wyrzykowski, D.; Ciupak, O.; Demkowicz, S.; Izadi, F.; Denifl, S.; Rak, J. Surprising Radiolytic Stability of 8-Thiomethyladenine in an Aqueous Solution. *J. Phys. Chem. B* **2024**, *128*, 3621–3630. [CrossRef] [PubMed]
14. Kocábková, B.; Ďurana, J.; Rakovský, J.; Poterya, V.; Fárník, M.; Gatt, M.; Schöpfer, G.; Jung, P.; Ončák, M. Electron attachment to CH_3COCl molecule and clusters. *RSC Adv.* **2025**, *15*, 23983–23993. [CrossRef] [PubMed]
15. Kopyra, J.; Wierzbicka, P.; Abdoul-Carime, H. Electron-Induced Fragmentation of 5-Iodouridine: Implications for Enhanced Radiotherapy. *J. Phys. Chem. Lett.* **2025**, *16*, 10536–10541. [CrossRef] [PubMed]
16. Das, S.; Lyshchuk, H.; Chaudhary, A.; Saha, S.; Kočišek, J.; McElwee-White, L.; Fedor, J.; Nag, P. Electron-induced dissociation of iron tetracarbonyl acrolein. *J. Phys. B* **2026**, *59*, 035201. [CrossRef]
17. Mendes, M.; Tafrishi, R.; Guerra, P.; Holzmeier, F.; Ingólfsson, O.; da Silva, F.F. Pathways to high-performance extreme ultra-violet lithography resists: Dissociative electron attachment to pentafluoro-phenyl triflate. *iScience* **2025**, *28*, 114020. [CrossRef] [PubMed]
18. IDEADB—Innsbruck Dissociative Electron Attachment Database. re3data.org: IDEADB; Editing Status 22-03-2023; re3data.org—Registry of Research Data Repositories. Available online: https://doi.org/10.17616/R3F34C (accessed on 27 April 2026).
19. Pitchford, L.C.; Alves, L.L.; Bartschat, K.; Biagi, S.F.; Bordage, M.-C.; Bray, I.; Brion, C.E.; Brunger, M.J.; Campbell, L.; Chachereau, A.; et al. LXCat: An Open-Access, Web-Based Platform for Data Needed for Modeling Low Temperature Plasmas. *Plasma Process. Polym.* **2017**, *14*, 1600098. [CrossRef]
20. Carbone, E.; Graef, W.; Hagelaar, G.; Boer, D.; Hopkins, M.M.; Stephens, J.C.; Yee, B.T.; Pancheshnyi, S.; van Dijk, J.; Pitchford, L. Data Needs for Modeling Low-Temperature Non-Equilibrium Plasmas: The LXCat Project, History, Perspectives and a Tutorial. *Atoms* **2021**, *9*, 16. [CrossRef]
21. Van Dijk, J.; Boer, D. LXCat 3 and beyond—Fostering reproducibility in low-temperature plasma science. *Publ. Astron. Obs. Belgrade* **2024**, *103*, 100. [CrossRef]
22. Hoshino, M.; Limão-Vieira, P.; Probst, M.; Nunes, Y.; Tanaka, H. Dissociative electron attachment to carbonyl fluoride, F_2CO. *Int. J. Mass Spectrom.* **2011**, *303*, 125–128. [CrossRef]
23. Matias, C.; Mauracher, A.; Huber, S.E.; Denifl, S.; Limão-Vieira, P.; Scheier, P.; Märk, T.D.; González-Méndez, R.; Mayhew, C.A. Dissociative electron attachment to the volatile anaesthetics enflurane and isoflurane and the chlorinated ethanes pentachloroethane and hexachloroethane. *Int. J. Mass Spectrom.* **2015**, *379*, 179–186. [CrossRef]
24. Kopyra, J.; Marinković, B.P.; Maljković, J.B. Investigation of the anaesthetic isoflurane fragmentation induced by electron impact. *Eur. Phys. J. D* **2025**, *79*, 97. [CrossRef]

25. Shiraishi, Y.; Ikeda, K. Uptake and biotransformation of sevoflurane in humans: A comparative study of sevoflurane with halothane, enflurane, and isoflurane. *J. Clin. Anesth.* **1990**, *2*, 381–386. [CrossRef] [PubMed]
26. Espinosa, S.; Martínez, F.; Antiñolo, M.; Nielsen, O.J.; Jiménez, E. Updated global warming potentials of inhaled halogenated anesthetics, isoflurane and sevoflurane from new temperature dependent OH-kinetics. *Environ. Sci. Process. Impacts* **2025**, *27*, 2410–2421. [CrossRef] [PubMed]
27. Lange, E.; da Silva, F.F.; Jones, N.C.; Hoffmann, S.V.; Duflot, D.C.; Limão-Vieira, P. The lowest-lying electronic states of isoflurane and sevoflurane in the 5.0–10.8 eV energy range investigated by experimental and theoretical methods. *Chem. Phys. Lett.* **2019**, *716*, 42–48. [CrossRef]
28. Sulbaek Andersen, M.P.; Nielsen, O.J.; Karpichev, B.; Wallington, T.J.; Sander, S.P. Atmospheric chemistry of isoflurane, desflurane, and sevoflurane: Kinetics and mechanisms of reactions with chlorine atoms and OH radicals and global warming potentials. *J. Phys. Chem. A* **2012**, *116*, 5806–5820. [CrossRef] [PubMed]
29. Humbert, D.; Braams, B. XSAMS: XML Schema for Atomic and Molecular Data and Particle Solid Interactions. In *Summary Report of an IAEA Consultants' Meeting, Vienna, Austria, 10–11 September 2009*; NDC(NDS)-0562; International Atomic Energy Agency (IAEA): Vienna, Austria, 2010. [CrossRef]
30. Regandell, S.; Marquart, T.; Piskunov, N. Inside a VAMDC data node—Putting standards into practical software. *Phys. Scr.* **2018**, *93*, 035001. [CrossRef]
31. Vukalović, J.; Marinković, B.P.; Rosado, J.; Blanco, F.; García, G.; Maljković, J.B. Investigating Theoretical and Experimental Cross Sections for Elastic Electron Scattering from Isoflurane. *Phys. Chem. Chem. Phys.* **2024**, *26*, 985–991. [CrossRef] [PubMed]
32. Vujčić, V.; Srećković, V.; Marinković, B. *sambolino/acol*, version 2.0.0; ACol: DEA Support, Data Model and Interface Redesign; Zenodo: Geneva, Switzerland, 2026. [CrossRef]
33. Silva, T.; Lobo, V.S.; Pereira-da-Silva, J.; Ferreira da Silva, F. Dissociative Electron Attachment Prediction of Halogenated Organic Molecules Using Machine Learning. *ACS Omega* **2026**, *11*, 22082–22092. [CrossRef] [PubMed]
34. Stokes, P.W.; White, R.D.; Campbell, L.; Brunger, M.J. Toward a complete and comprehensive cross section database for electron scattering from NO using machine learning. *J. Chem. Phys.* **2021**, *155*, 084305. [CrossRef] [PubMed]

Disclaimer/Publisher's Note: The statements, opinions and data contained in all publications are solely those of the individual author(s) and contributor(s) and not of MDPI and/or the editor(s). MDPI and/or the editor(s) disclaim responsibility for any injury to people or property resulting from any ideas, methods, instructions or products referred to in the content.